Blur-Mask Approach for Real-Time Calculation of Light Spreading Function (LSF) on Spatial Modulated High Dynamic Range LCDs

Lin-Yao Liao and Yi-Pai Huang

***Abstract*—Blur-mask approach (BMA) was developed to simulate the light distribution of locally controlled LED backlight, providing much lower computational complexity which is less than 1% of that of conventional convolution approach and being successfully demonstrated on a 37" high dynamic range (HDR) LCD-TV with real-time modification to perform high quality image (Less image distortion) and high contrast ratio (∼ 20,000:1 with test image-Lily).**

I. Introduction

LIQUID crystal displays (LCDs) have become popular monitor/TV option because of their light weight, high resolution, good color performance, and other features. However, a drawback to conventional LCDs is a poor image contrast ratio (about 1200:1) due to light leakage from liquid crystals and a pair of non-ideal cross polarizers. After high dynamic range LCD (HDR-LCD) were proposed, the backlight signal could be modulated to much enhance the contrast ratio upon the locally controlled backlight [1]–[3]. The backlight (BL) distribution, however, is no longer a uniform brightness, which will affect the observed image brightness and might cause some image distortion. Therefore, the image signals have to be adjusted to compensate the brightness and keep the image details.

Conventionally, BL distribution is simulated by convolving the BL signals with the light spread function (LSF) which represents the spatial intensity distribution of each LED segment. According to the convolution result, the compensated image signals are derived, and an HDR image can be displayed by combining the BL distribution and the compensated image signals [4]–[7]. Fig. 1 shows the flowchart of the algorithm. The step, BL simulating, described before is the most complex step and dominating the complexity of the system. Therefore, how to simplify the step of BL simulating is the key point to make an HDR system work in real-time.

The convolution approach, however, needs huge computational complexity and the storage of the LSF which will also result in a very high hardware loading, especially for full-HD images. For conventional hardware, it is not easy to perform in real-time. Thus, a novel method named blur-mask approach (BMA) was proposed to approximate the backlight distribution which can much reduce the computational complexity and has been demonstrated the HDR-images can be real-time modified to perform high quality images, especially for TV applications.

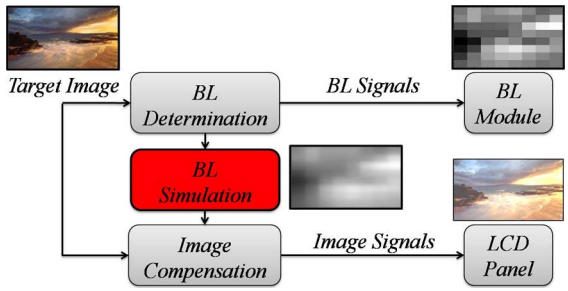

Fig. 1. Main flow of the algorithm to obtain an HDR image.

II. Blur-Mask Approach (BMA)

A. Concept of BMA—Multi-Step Calculation

The main concept of Blur-mask approach (BMA) was to utilize a low-pass-filter (LPF) to blur the original backlight image which is used to simulate the light spreading of backlight. The size and values of the original backlight image is determined by the number of divided BL segments and driving values of each BL segment in gray-level. By several steps of expanding and blurring, the distribution of this gray-level image will be approximate to the real backlight distribution. Subsequently, divide the target image by the blurred backlight image and take gamma effect (ã) of the display device into consideration [8], the compensation image signals can be obtained.

As shown in Fig. 2, the backlight unit of a full-HD 1920×1080 37" LCD was designed as 8×8 segments, the first step is to determine the corresponding BL signals and obtain the original backlight image whose size is 8×8 pixels. Second, the length and width of the 8×8 image is expanded by a factor of 2 to a 16×16 image which the way of expanding is linear up-scaling without any process.

After the expanding, convolve the 16×16 image by a LPF which the filter size is set as 3×3 and the filter kernel, a, is equal to b/m and c/n, as shown in Fig. 3 and (1),

$$S = \left\{ (m,n) \middle| \left(m = \frac{b}{a}, n = \frac{c}{a} \right) \cap 0 \le m,n \le 1 \right\} \quad (1)$$

Manuscript received February 04, 2009; revised September 16, 2009. Current version published March 16, 2010. This work was supported by National Science Council, Taiwan, under Contract NSC 96-2221-E-009-113-MY3.

The authors are with the Department of Photonics & Institute of Electro-Optical Engineering/Display Institute National Chiao Tung University, Hsinchu, Taiwan, 300 (e-mail: finalhome.eo95g@nctu.edu.tw; boundshuang@mail.nctu.edu.tw).

Color versions of one or more of the figures in this paper are available online at http://ieeexplore.ieee.org.

Digital Object Identifier 10.1109/JDT.2009.2035826

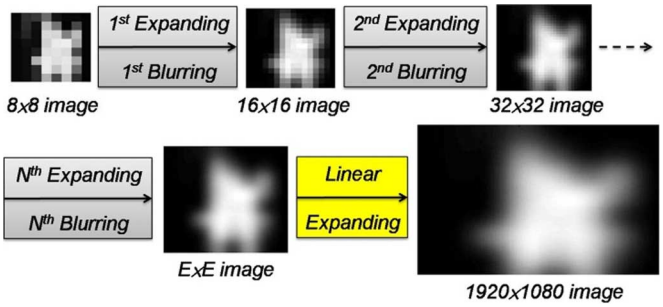

Fig. 2. Target images and the procedure of expanding and blurring in BMA.

c	b	c
b	a	b
c	b	c

Fig. 3. The 3×3 low-pass filter.

TABLE I
PARAMETERS OF BLUR-MASK APPROACH

	Definition
a, b, c	*Filter Coefficients*
m, n	*Filter Modulators*
N	*The number of expanding and blurring steps to E×E blurred-image*
E	$E=8\times 2^{N}$

where b, and c are the coefficients of the filter and m, n module the filter coefficients, a, b, and c.S_{Mask} is the set of LPF modulator, defining the coefficients of LPF, a, b, and c. For the convergence, $a+4b+4c$ has to be equal to 1. Repeat the expanding and blurring $\boldsymbol{N}$ times until the size of blurred image is expanded to $\boldsymbol{E}\times\boldsymbol{E}$, where $\boldsymbol{E}=8\times 2^{N}$. Finally, this $\boldsymbol{E}\times\boldsymbol{E}$ blurred-image is expanded to 1920×1080 for a resolution of HDTV to represent the BL distribution for image signals compensation.

The $\boldsymbol{E}$ value can be investigated to make the difference between the final 1920×1080 image with and without blurring be small enough to avoid a large number of hardware loading due the last step of blurring. In our experiments, when $\boldsymbol{E}$ value is equal and larger than 256, the error of BL simulation between these two case can be ignored.

B. Modified BMA—Single-Step Calculation With Look-Up Table

Actually, the several steps of expanding and blurring of BMA process can be simplified, and converted into a single-step calculation. Consider the expanding and blurring between two steps,

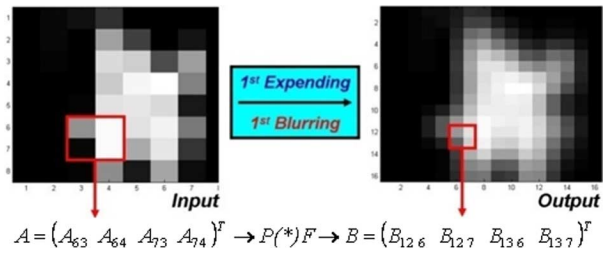

Fig. 4. An example of expending and blurring between two steps in the case of that $K=1$, $(i,j)=(6,3)$, and $(I,J)=(12,6)$ in a matrix form.

the calculation analysis can be represented in a matrix form, shown in (2) at the bottom of the page, where matrices A and B are 4 values of BL images between 2 steps, as shown in Fig. 2. Matrix F describes the a, b, and c values of a LPF, and the suffixes (I,J) and (i,j) in matrix B and $P(A)$ denote the pixel sites of the output image and input image, respectively. $P(A)$ is a permutation matrix function which can arrange matrix A into a 4×4 matrix as shown above. An example in the case of that step 1 (8×8 matrix) and step 2 (16×16 matrix) as shown in Fig. 4, $(i,j)=(6,3)$, and $(I,J)=(12,6)$, 4 output values in the blurred image of step 2 can be calculated by 4 input values in step 1, and the matrixes, $P(*)$, and F which is illustrated clearly in Fig. 4.

Substitute A^* which denotes 4 neighboring values in the BL image of step $*$ for A and B, the calculations between steps can be expressed following:

$$\begin{aligned} P(A_1)F &= A_2 \\ P(P(A_1)F)F &= A_3 \\ &\vdots \\ \underbrace{P(P\ldots(P}_{N}(A_1)\underbrace{F)\ldots F)F}_{N} &= A_N \Rightarrow T_N(A_1) \\ &\equiv \underbrace{P(P\cdots(P}_{N}(A_1)\underbrace{F)\cdots F)F}_{N} \\ &= A_N \end{aligned} \tag{3}$$

suffixes (I,J) in matrix A^N here are equal to 2^N times of (i,j) in matrix A_1 due to the $\boldsymbol{N}$ times expanding. Therefore, input 4 neighboring values of step 1 to the function $T_N(*)$, a set of 4 neighboring values of the step $\boldsymbol{N}$ can be calculated in single-step.

A look-up table (LUT) whose size is $2^N\times 2^N\times \boldsymbol{M}^2$ values has been established upon the above concept, where $\boldsymbol{M}$ is the length of the LPF. By this LUT, the final result can be obtained directly, as shown in Fig. 5. For the case of $\boldsymbol{M}=3$,

$$B=P(A)F\Rightarrow\begin{bmatrix} B_{IJ} \\ B_{IJ+1} \\ B_{I+1J} \\ B_{I+1J+1}\end{bmatrix}=\begin{bmatrix} A_{ij}A_{ij+1} & A_{i+1j} & A_{i+1j+1} & \\ A_{ij+1} & A_{i+1j+1} & A_{ij} & A_{i+1j} \\ A_{i+1j} & A_{ij} & A_{i+1j+1} & A_{ij+1} \\ A_{i+1j+1} & A_{i+1j} & A_{ij+1} & A_{ij}\end{bmatrix}\begin{bmatrix}(a+2b+c) \\ (b+c) \\ (b+c) \\ c\end{bmatrix} \tag{2}$$

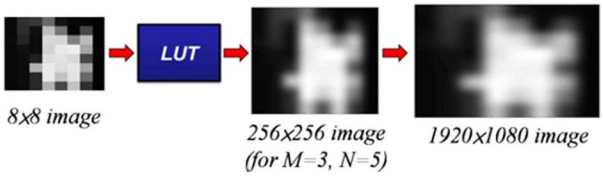

Fig. 5. Single-step calculation of BMA performed by a look-up table.

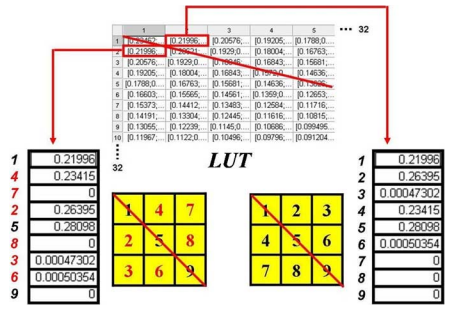

Fig. 6. Symmetry and repetition of the look-up table with single-step calculation.

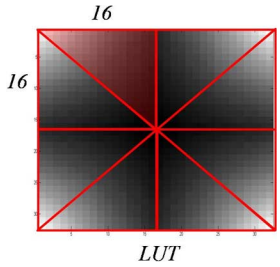

Fig. 7. Whole coefficients of the LUT can be represented with only the 1/8 original size.

and $\boldsymbol{N} = 5$, a 256×256 blurred image is calculated by a LUT in single-step, and expand this 256×256 image linearly to a 1920×1080 resolution. This final result is utilized for image signals compensation.

C. Further Simplification of Look-up Table in BMA

In practice, there are many repetitions and symmetries in the derived LUT due to the symmetry of the utilized LPF, which means the size of LUT actually stored in hardware is no longer $2^N \times 2^N \times \boldsymbol{M}^2$ values. Fig. 6 shows the symmetry and repetition of the LUT. Each couple of cells which is symmetric by the diagonal has all the same coefficients whose order is re-arranged in the same way of symmetry, as shown as the order of the yellow squares in Fig. 6. Not only the diagonal but also the other diagonal and two horizontal and vertical centerlines, these symmetry and repetition also obey. As a result, the size of the LUT, $2^N \times 2^N \times \boldsymbol{M}^2$, can be reduced down to $\left\{\left[(2^{N-1}+1) \times 2^{N-1}\right]/2\right\} \times \boldsymbol{M}^2$ which is about 1/8 of original size, as shown in Fig. 7. For an $\boldsymbol{M} = 3$ and $\boldsymbol{N} = 5$ case, only 1,224 values are needed to be stored in hardware to perform BMA (Conventional convolution approach for full-HD required $\sim$1920$\times$1080 values storing).

D. Computational Complexity

BMA can provide a significant reduction in computational complexity and hardware loading, especially when the LUT is

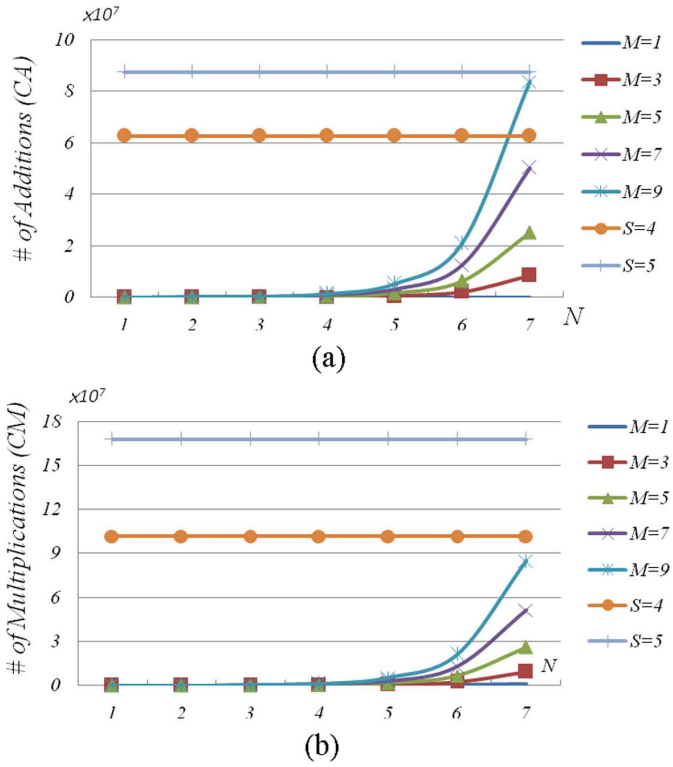

Fig. 8. Computational comparison of the two algorithms by different $\boldsymbol{M}$, $\boldsymbol{N}$, $\boldsymbol{S}$ in (a) the number of addition(CA), and (b) multiplication(CM), where $\boldsymbol{M}$, $\boldsymbol{N}$, and $\boldsymbol{S}$, represent the filter size, expanding steps, and parameter describing the size of chosen LSF.

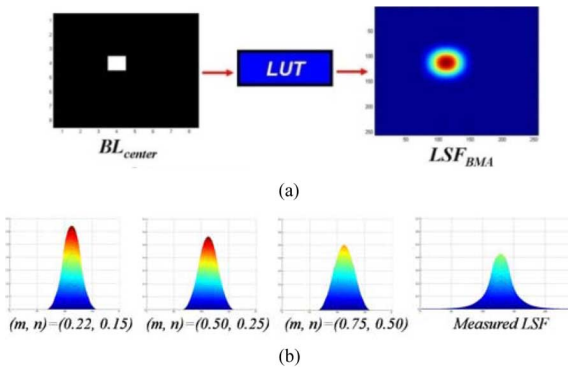

Fig. 9. (a) Impulse response of the LUT, and (b) the $LSF_{\mathrm{BMA}}s$ with different $(\boldsymbol{m}, \boldsymbol{n})$.

further simplified. To quantify the improvement between BMA and convolution one, the computation is divided into additions (CA) and multiplications (CM) parts, and their graphs for different $\boldsymbol{M}$, $\boldsymbol{N}$, and $\boldsymbol{S}$ are illustrated in Fig. 8, where $\boldsymbol{S}$ is the parameter describing the size of chosen LSF. Actually, convolution approach can not generate a smooth backlight distribution until $\boldsymbol{S}$ is larger than 5 due to the defect edge of the LSF, which leads to a 2,624,400-value storage of LSF and 87,609,600 additions and 167,961,600 multiplications requirement at least. In comparison, for BMA, the case of $\boldsymbol{M} = 5$ and $\boldsymbol{N} = 5$ can yield an acceptable image quality. Only a 3,400-value LUT is required to store in hardware, and 1,572,864 additions and 1,638,400 multiplications are needed to calculate the backlight

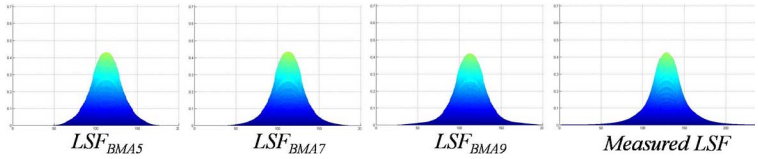

Fig. 10. $LSF_{\mathrm{BMA}}s$ generated by different optimized LPFs of 5 × 5, 7 × 7, and 9 × 9 filter sizes compared with the measured LSF.

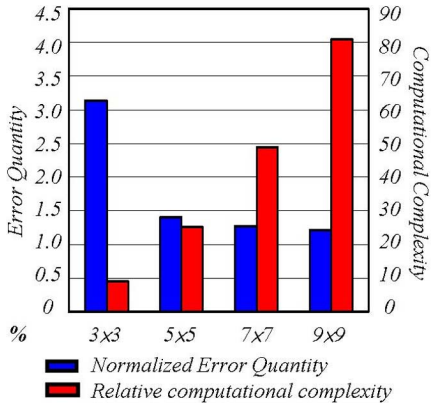

Fig. 11. Normalized error quantity and relative computation complexity by different LPF size.

distribution per frame, which is just about 1% of convolution one.

III. Blur Mask Optimization

A. Impulse Response of LUT

To optimize the results of BMA, adjusting the $(\boldsymbol{m},\boldsymbol{n})$ values can generate different LPF to make the results of BMA be approximate to a real backlight distribution. An impulse response named LSF_{BMA} yielded by performing BMA with a pulse input which denotes a 255 gray level on the center of BL segments named BL_{center} can be used to analysis, as shown in Fig. 9(a). Fig. 9(b) illustrates the $LSF_{\mathrm{BMA}}s$ generated by different LUTs derived by the sets of $(\boldsymbol{m},\boldsymbol{n})$ values, and the LSF_{BMA} generated by a set of optimized $(\boldsymbol{m},\boldsymbol{n}) = (\mathbf{0.75},\mathbf{0.5})$ (i.e., a, b, and c are 0.1667, 0.125, and 0.083 respectively) can has an more approximate normalized intensity to the measured LSF, but the distribution cannot be spread out. Definitely, the larger size of LPF utilized to perform BMA, the more approximate LSF_{BMA} to a measured LSF can be obtained, but the complexity of the LPF optimization, the size of LUT stored, and the computational complexity of BMA process also get higher. Fig. 10 shows the $LSF_{\mathrm{BMA}}s$ generated by different size of optimized LPFs, and the suffixes of $LSF_{\mathrm{BMA}}s$ donate the size of LPFs utilized. Not only the distribution but also the normalized intensity can be approximate to a measure one as the larger size of optimized LPF applied. However, if the defects of asymmetric light distribution of the BL segment are taken into consideration, the analysis would be more complicated.

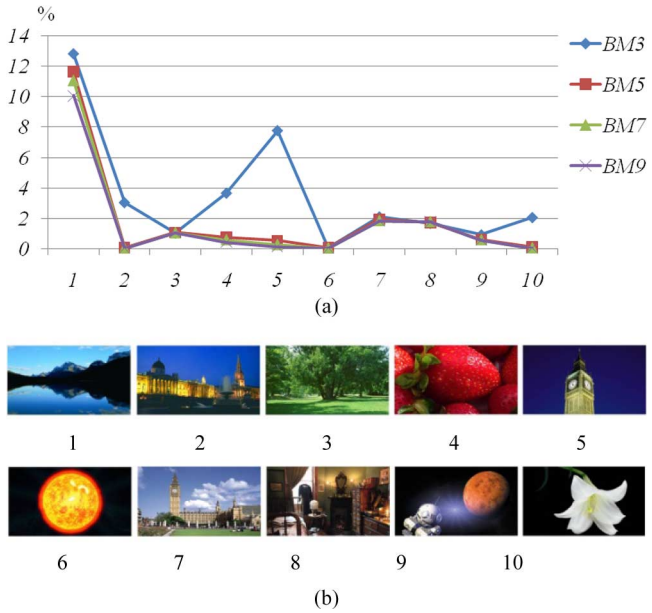

Fig. 12. (a) Calculated color difference of 10 test images between the results of BMA and convolution by CIEDE2000, and (b) corresponding test images.

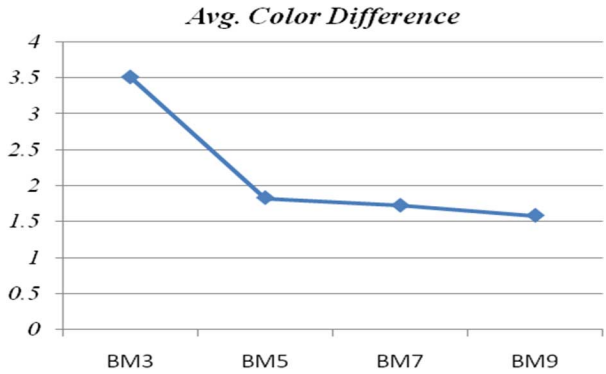

Fig. 13. Average color difference of 10 test image by BMA of using 3 × 3, 5 × 5, 7 × 7, and 9 × 9 LPFs.

B. Error Quantification and Image Quality

To quantify the difference between a LSF_{BMA} and a measured LSF, an error quantity, *Diff* function, can be applied, as shown in

$$Diff = \sum_{x,y}(\mathrm{LSF}_{\mathrm{BMA}} - \mathrm{LSF})^2 \tag{4}$$

where x, and y indicate the dimension of LSF_{BMA} and the measured LSF. The relative computational complexity by different size of optimized LPFs is also taken in to consideration, and the graph is shown in Fig. 11. The relation between the error

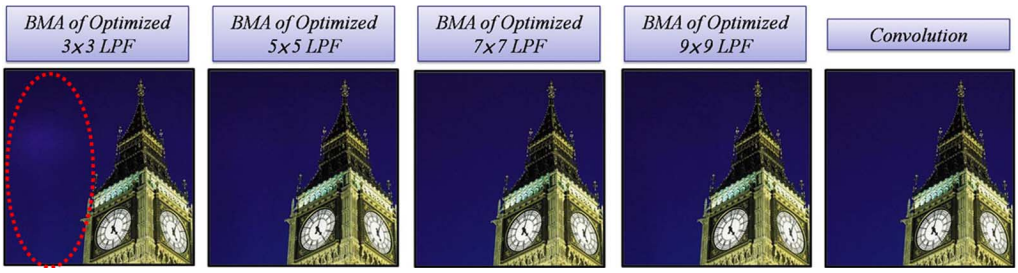

Fig. 14. Results of test image5 calculated by 3×3, 5×5, 7×7, 9×9 optimized LPFs, and convolution method. The result of 3×3 LPF shows an incorrect compensation in the blue sky near the tower.

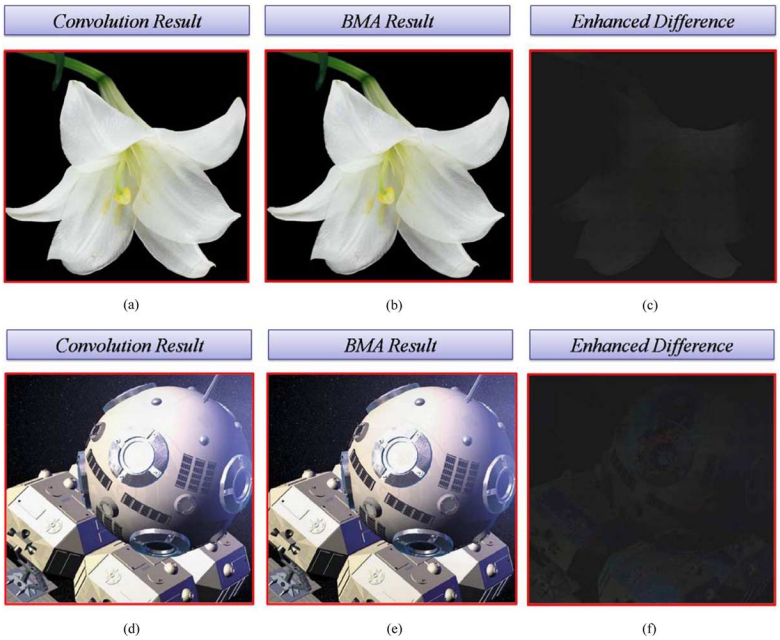

Fig. 15. Partly magnified results of test image, *Lily* and *Space Robot*. (a), (d) The enhanced difference between the results of Convolution and that of BMA, (b), (e) the results of convolution, and (c), (f) that of BMA respectively.

quantity and computational complexity is a trade-off case. The larger LPF with the lower error quantity can be obtained, but the hardware loading also get higher. However, when the LPF size reaches to exceed 5×5, error quantity begins to saturate and the complexity is getting higher.

In order to verify the performance of optimized $LSF_{\mathrm{BMA}}s$ in image quality, 10 test images are evaluated and the difference between the results of BMA and that of convolution are quantified by CIEDE2000 [9]–[11], which was designed for predicting the visual difference for large isolated patches and often desired to determine the perceived difference of color images. Fig. 12(a) shows the results of color difference by optimized 3×3, 5×5, 7×7, and 9×9 LPFs, and the results are indicated by BM3, BM5, BM7, and BM9. All of the BL signals are determined by Inverse-of-Mapping Function (IMF) method which was proposed to optimize the BL signals frame by frame [12]. The numbers on the vertical axis are the percentage of the number of pixels which the color difference between the results of BMA and convolution are larger than 3. The color difference is acceptable under less than 3 of CIEDE2000 is concluded by our human experiments. Fig. 12(b) shows the corresponding images to the numbers on the horizontal axis in Fig. 12(a) including high contrast ratio, high color saturation, and complicate images. Through the results of calculating the color difference, most of the images are acceptable and only a small number of pixels can be distinguished the difference except utilizing 3×3 LPF. Although test image1 has lager percentage that the color difference exceeds 3, the average color difference is still less than 1.5.

TABLE II
SPECIFICATION OF THE EXPERIMENTAL DEVICE

Specification	
Device	*HDR-LCD*
Backlight Module	*8x8 RGB LED Segments*
Resolution	*1920x1080*
LC Mode	*MVA*

Calculating the average color difference of 10 test images by utilizing 3×3, 5×5, 7×7, and 9×9 optimized LPFs, Fig. 13 illustrates a similar trend to Fig. 11 which the color difference stars to saturate as 5×5 LPFs is applied. The results of test image5 calculated by optimized LPFs are shown in Fig. 14. All of the results can display a uniform blue sky near the tower except that of 3×3 LPF due to the serious incorrect

TABLE III
THE DISTORTION RATIO, BRIGHTNESS, CONTRAST RATIO AND COMPUTATIONAL COMPLEXITY OF TEST IMAGES, *LILY* AND *PLANATE* COMPENSATED BY CONVOLUTION, AND BMA

	Lily					*Space Robot*				
	ΔE00	*Lmax*	*CR*	*Computation*		*ΔE00*	*Lmax*	*CR*	*Computation*	
Conv.	*0.27*	*431.5*	*21575*	*CM*	*100.00%*	*0.11*	*463.0*	*3858*	*CM*	*100.00%*
				CA	*100.00%*				*CA*	*100.00%*
BMA	*0.56*	*396.6*	*19830*	*CM*	*0.98%*	*0.53*	*462.3*	*3853*	*CM*	*0.98%*
				CA	*1.80%*				*CA*	*1.80%*

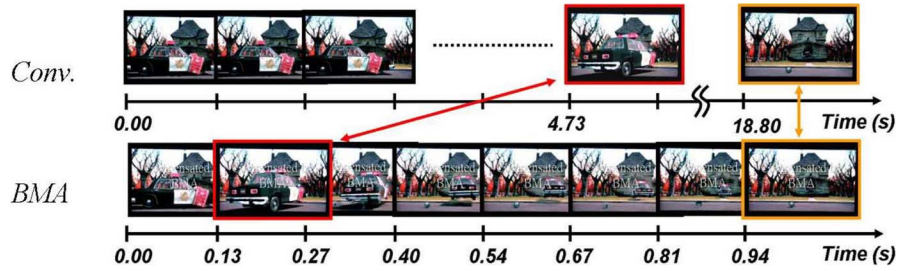

Fig. 16. Time difference of the displayed video with image compensation by convolution approach and BMA.

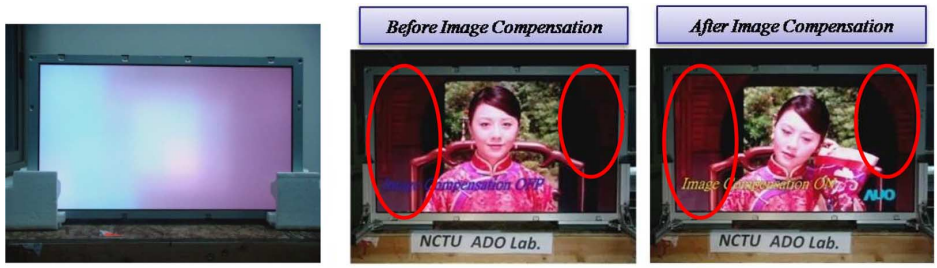

(a) (b)

Fig. 17. Real-time demo of HDR system. (a) The dynamic BL distribution of the HDR system (Media 1). (b) The real-time image compensation by BMA. The image was captured in real demo video (Media 2).

LSF_{BMA3}. Therefore, 5×5 mask could be a balance result for image quality and hardware implementation.

To investigate the performance of BMA and convolution, Table III illustrates the measurement results of test image, *Lily* and *Space Robot* (ie. test image10 and test image9) displayed by 37" HDR-LCD. The specification of HDR panel is list in Table II. Image signals were compensated by using two algorithms, convolution (Conv.) with $\boldsymbol{S} = 5$ and BMA with the optimized 5×5 LPF, and BL signals were also determined by IMF. Four main parameters, average color difference with target image ($\Delta E00$), maximum luminance ($L_{\max}$), contrast ratio (*CR*), and computational complexity were discussed. The result shows BMA and provide a very low $\Delta E00$ with target image which means the compensated results are very close to the target. Furthermore, BMA also maintains a very high contrast ratio ($\sim$ 20,000:1 of test image—Lily), and has similar maximum luminance to that of convolution. The most significance is the computational complexity of BMA was dramatically reduced down to about 1% of convolution one which means BMA can be easily applied for "real-time" TV application.

The magnified image of the results and the enhanced difference are shown in Fig. 15. From Fig. 15(a), (b), (d), and (e), the image quality of BMA is almost the same as that of convolution. Fig. 15(c) and (f) shows the enhanced difference which is directly subtracting the results of BMA from that of convolution and enhancing the data values. The difference are almost cannot be visible, especially in the real image or displayed in real-time, which also demonstrates that BMA is feasible to simulate the backlight distribution for HDR-LCD.

C. Real-Time Improvement

A video was displayed by the HDR-LCD, and the image signals were compensated by convolution approach and BMA respectively. The played videos were captured by a camcorder, and the analyzed image frames are shown in Fig. 16. The frames marked by the arrows indicate the same frames of the video. Obviously, the display speed of convolution one is very slow and shows a serious lag. On the other hand, BMA can provide a real-time performance which keeps the original video display fluently. Another real-time demo describing the light distribution of the BL module and the HDR-TV with and without image compensation by using BMA is show in Fig. 17. In this real-time demo, Fig. 17(a) (Media 1) shows the R, G, B dynamic BL [13], [14] distribution of the HDR system which is different from the traditional full-on LCD system, and Fig. 17(b) (Media 2) shows

that operating BMA according to the BL distribution can obviously enhance image details in the dark region (especially the highlighted dash region), and the image brightness also can be kept.

IV. Conclusion

A real-time calculation method of light spreading function (LSF), named blur-mask approach (BMA), for high dynamic range liquid crystal displays (HDR-LCDs) was proposed. BMA utilizes a low-pass filter to blur the original backlight gray-level image. By expanding and blurring, the BMA result can be used to represent the backlight distribution for image signals compensation. Through the simplification of single-step process, BMA for hardware implement can be applied as a look-up table (LUT) with 3400 values only under the condition of utilizing a 5×5 low-pass filter, and has about 1% hardware calculation loading compared to that of convolution approach. Due to the simplicity, BMA was successfully demonstrated on a 37" HDR-LCD for processing in real-time modification to yield high image quality, such as less image distortion, high contrast, and high brightness, for future high quality TV applications.

Acknowledgment

The author would like to acknowledge S.-C. Yeh, AU Optronics Corporation (AUO), Hsinchu, Taiwan, for their support on the 37-in RGB LED Backlight HDR-LCD TV.

References

[1] H. Seetzen, W. Heidrich, W. Stuerzlinger, G. Ward, L. Whitehead, M. Trentacoste, A. Ghosh, and A. Vorozcovs, "High dynamic range display systems," *ACM Trans. Graphics*, vol. 23, no. 3, pp. 760–768, 2004.

[2] H. Seetzen, L. A. Whitehead, and G. Ward, "A high dynamic range display using low and high resolution modulators," in *Proc. SID Symp. Dig.*, 2003, vol. 34, pp. 1450–1453.

[3] E. Y. Oh, S. H. Baik, M. H. Sohn, K. D. Kim, H. J. Hong, J. Y. Bang, K. J. Kwon, M. H. Kim, H. Jang, J. K. Yoon, and I. J. Chung, "IPS-mode dynamic LCD-TV realization with low black luminance and high contrast by adaptive dynamic image control technology," *J Soc. Inf. Display*, vol. 13, pp. 215–219, 2005.

[4] Y. W. Wang, Y. K. Cheng, H. P. D. Shieh, T. M. Wang, and H. W. R. Lin, "Analyses of point spread function in high dynamic range display system," *Opt. Photon. Taiwan* , 2005.

[5] H. Chen, J. Sung, T. Ha, and Y. Park, "Locally pixel-compensated backlight dimming on LED-backlit LCD TV," *J. Inf.. Display*, vol. 15, pp. 981–988, 2007.

[6] F. Li, X. Feng, I. Sezan, and S. Daly, "Two approaches to derive LED driving signals for high-dynamic-range LCD backlights," *J. Inf. Display*, vol. 15, pp. 989–996, 2007.

[7] C. H. Chen and H. P. D. Shieh, "Effects of backlight profiles on perceived image quality for high dynamic range LCDs," *J. of Display Technology*, vol. 4, no. 2, pp. 153–159, 2008.

[8] L. Kerofsky and S. Daly, "Brightness preservation for LCD backlight dimming," *J. Inf. Display*, vol. 14, pp. 1111–1118, 2006.

[9] *Improvement to Industrial Colour-Difference Evaluation*. Vienna, Austria: CIE, CIE Publication, Central Bureau of the CIE, 2001.

[10] G. M. Johnson and M. D. Fairchild, "A top down description of S-CIELAB and CIEDE2000," *Color Res. Appl.*, vol. 28, pp. 425–435, 2003.

[11] M. R. Luo, G. Cui, and B. Rigg, "The development of the CIE 2000 colour difference formula," *Color Res. Appl.*, vol. 26, no. 5, pp. 340–350.

[12] F. C. Lin, L. Y. Liao, C. Y. Liao, Y. P. Huang, H. P. D. Shieh, T. M. Wang, and S. C. Yeh, "Dynamic backlight gamma on high dynamic range LCD TVs," *J. Display Technol.*, vol. 4, no. 2, pp. 139–146, 2008.

[13] G. Z. Wang, F. C. Lin, Y. P. Huang, and H. P. D. Shieh, "Delta-Color adjustment method for color controlled backlight of high dynamic range LCD-TVs," in *Proc. SID Symp. Dig.*, 2008, vol. 39, pp. 768–771.

[14] Y.-L. Chen, Y.-K. Cheng, Y.-P. Huang, H.-P. D. Shieh, and S.-C. Yeh, "Color optimization model for high dynamic range LCDs with RGB color backlights," in *Proc. SID Symp. Dig.*, 2009, vol. 43, pp. 636–639.

Lin-Yao Liao received the B.S. degree from Department of Electrical Engineering, National Sun Yat-sen University, Kaohsiung, Taiwan, in 2006. He is working toward the Ph.D. degree at Department of Photonics, Institute of Electro-Optical Engineering, National Chiao Tung University, Hsinchu, Taiwan.

His current research is including high image-quality with low power consumption LCDs, and optical design with liquid crystal lenses.

Yi-Pai Huang received the B.S. degree from National Cheng-Kung University in 1999, and the Ph.D. degree (with merit) from the Institute of Electro-Optical Engineering, National Chiao Tung University (NCTU), Hsinchu, Taiwan.

He is currently an assistant professor in the Department of Photonics & Display Institute, National Chiao Tung University, Hsinchu, Taiwan. He was a project leader in the technology center of AUOptronics (AUO) Corporation. From 2001 to 2002, he had been an intern at the Photonics and Communications Laboratory, the School of Optics/CREOL, University of Central Florida (UCF).

He was awarded the 2001 SID Best Student Paper Award, 2004 SID distinguished student paper award, 2005 Golden Thesis Award of Acer Foundation, and 2005 AUO Bravo Award. He had successfully developed "advanced-MVA LCD" for the next generation products of AUO in 2005. His current research interests are advanced display systems (High dynamic range LCD and Field sequential LCD), display human vision evaluation, 3-D displays, and display optics. He has published 7 journal papers, 20 international conference papers, and has 11 U.S. patents (5 granted, 6 pending) to his credit.